1 **Title:** FGF-2 Stimulates the Growth of Tenogenic Progenitor Cells to Facilitate the Generation of

2 *Tenomodulin*-positive Tenocytes in a Rat Rotator Cuff Healing Model

3

4 **Running title:** Effect of FGF-2 on Rotator Cuff Healing

5

6

7   **Abstract**

8   **Background**: Fibroblast growth factor (FGF)-2 has the potential to enhance tendon-to-bone healing

9   after rotator cuff (RC) injury.

10   **Hypothesis:** FGF-2 stimulates tenogenic differentiation of progenitors to improve the biomechanical

11   strength and histological appearance of repaired RCs in rats.

12   **Study Design:** Controlled laboratory study.

13   **Methods:** Adult male Sprague-Dawley rats (n = 156) underwent unilateral surgery to repair the

14   supraspinatus tendon to insertion sites. The FGF-2-treated (gelatin hydrogel containing 5 μg of

15   FGF-2) and control groups (gelatin hydrogel only) were compared to investigate the effects of FGF-2

16   at 2, 4, 6, 8, and 12 weeks postoperatively. Biomechanical testing was performed at 6 and 12 weeks.

17   Semi-quantitative histological analysis and immunohistochemistry for the proliferating cell nuclear

18   antigen (PCNA) was performed, and the expression of tendon-related markers, including *Scleraxis*

19   (*Scx*) and *Tenomodulin* (*Tnmd*) were monitored by real-time reverse transcription polymerase chain

20   reaction (RT-PCR) and *in situ* hybridization. SRY-box containing gene 9 (Sox9) expression was

21   monitored by RT-PCR and immunohistochemistry. At 2 and 4 weeks, immunohistochemistry for

22   mesenchymal stem cell (MSC) markers were also performed.

23   **Results:** The FGF-2-treated group demonstrated a significant improvement in mechanical strength at

24   6 and 12 weeks and significantly higher histological scores than the control at ≥4 weeks. The average

25   incidence of PCNA-positive cells was significantly higher at 2 and 4 weeks, and more cells

26 expressing MSC markers were detected at the insertion site in the FGF-2-treated group. The

27 expression level of *Scx* increased significantly in the FGF-2-treated group from 4 to 8 weeks, while

28 the *Tnmd* level increased significantly from 4 to 12 weeks postoperatively. The localization of *Tnmd*

29 overlapped with the locations of reparative tissues accompanying collagen fibers with an aligned

30 orientation. The *Sox9* expression was significantly upregulated at 4 weeks in the FGF-2-treated

31 group.

32 **Conclusion:** FGF-2 promotes growth of the tenogenic progenitor cells, which participates in

33 tendon-to-bone healing, resulting in the biomechanical and histological improvement of repaired RC.

34 **Clinical Relevance:** These findings provide clues on the clinical development of regenerative repair

35 strategies for RC injury.

36 **Key Terms:** FGF-2, rotator cuff healing, *Scleraxis*, *Tenomodulin*, *Sox9*, cell proliferation, tenogenic

37 progenitors

38

What is known about the subject:

Rotator cuff (RC) tears are a common cause of shoulder pain and dysfunction that often require surgical repair. A relatively high repair failure rate (21.7%, 187/861 patients) was reported in a recent meta-analysis of 14 studies after RC surgical repair.[14] Various efforts (e.g., the application of growth factors or transplantation of mesenchymal stem cells) have been made to promote a reparative response.[7,8,9,24,28] Administration of the fibroblast growth factor 2 (FGF-2) has the potential to enhance the reparative response during the RC healing process;[9] however, little is known about the biological mechanism of the repair-promoting effect (improvement of biomechanical strength or histological appearance) by FGF-2 during RC healing.

What this study adds to existing knowledge:

In a rat model, the administration of FGF-2 to the healing tendon-bone interface after surgical repair of an acute supraspinatus injury improved the mechanical strength and histological appearance between the tendon and bone at ≥4 weeks. Moreover, the proliferation of cells expressing markers of mesenchymal stem cells was stimulated in the FGF-2-treated group during the early phase of RC healing. Subsequently, upregulation of the tendon markers such as *Scleraxis* (*Scx*) and *Tenomodulin* (*Tnmd*) were detected in the FGF-2-treated group at ≥4 weeks. Interestingly, localization of *Tnmd* mRNA overlapped with the locations of reparative tissues accompanying collagen fibers with an aligned orientation during RC healing.

58   This suggests that FGF-2 promotes the growth of tenogenic progenitor cells to participate in

59   tendon-to-bone healing, resulting in the histological and biomechanical improvement of RC healing.

60

Introduction

A rotator cuff (RC) injury is one of the most common causes of shoulder pain and dysfunction, often requiring surgical repair. Despite great improvement in surgical techniques for repairing RC tears, a recent meta-analysis of 14 studies reported on an imaging assessment of the structural integrity of RC repair, and it demonstrated a high rate of failed repair (21.7 %, 187/861 patients) at the latest follow-up.[14] Therefore, developing new strategies for enhancing tendon-to-bone healing is imperative.

Various growth factors are endogenously expressed during tendon-to-bone healing, suggesting that they play critical roles in the repair process,[27] and there is an interest regarding their use as therapeutic agents for enhancing RC repairs. Of those, fibroblast growth factor-2 (FGF-2) is a potent mitogen for a wide variety of cells, including mesenchymal stem cells (MSCs) and progenitor cells.[11, 19, 25] We previously demonstrated that the local administration of FGF-2 accelerates the initial tendon-to-bone healing as indicated by biomechanical tests and histological analyses after supraspinatus tendon repair in rats.[9] However, the biological mechanism of the reparative enhancement by FGF-2 during RC healing is unclear.

Recently, several genes have been identified as specific tendon markers. Scleraxis (Scx) is a basic helix-loop-helix transcription factor that is expressed in both tenogenic progenitors and tenocytes.[13, 15] Tenomodulin (Tnmd) is a type II transmembrane protein that is specifically expressed in the dense connective tissues such as tendons and ligaments.[17, 18] Tnmd is detected in mature tenocytes and is

6

80   positively regulated by Scx.[3, 18] Identification of these marker genes enables us to study the cellular

81   and molecular events that occur during the establishment of the osteotendinous junction in detail.

82   Recently, we reported that a subset of *Scx*-positive progenitors with an expression history of *SRY-box*

83   *containing gene 9* (*Sox9*) contributes to the formation of enthesis during development.[20]

84   The purpose of this study was to investigate the effects of FGF-2 administration on cell

85   proliferation and the expression of enthesis-related marker genes (i.e., *Scx*, *Sox9*, and *Tnmd*) during

86   RC tendon-to-bone healing in rats. The effects on biomechanical strength and histological

87   appearance during healing were also investigated. We hypothesized that FGF-2 stimulates the

88   tenogenic differentiation of progenitors and improves the biomechanical strength and histological

89   appearance of repaired RCs in rats.

90

Materials and Methods

Study Design

This study was approved by our institution's Animal Studies Committee and the Institutional Animal Care and Use Committee. We used a rat RC healing model, in which the supraspinatus tendon insertion site was transected and surgically repaired immediately, to investigate the effects of FGF-2 on tendon-to-bone healing. In this model, a normal tendon-to-bone insertion site is not regenerated even after 16 weeks postoperatively.[23]

We included 156 adult male Sprague-Dawley rats (19–21 weeks old; mean weight, 475 ± 37 g) that underwent unilateral surgery for supraspinatus tendon repair immediately after transaction, and they were randomly allocated to the control or FGF-2-treated groups (n = 78 per group). In the control, gelatin hydrogel sheets (MedGEL Co., Kyoto, Japan) with a phosphate-buffered saline (PBS) were applied between the supraspinatus tendon and bone. In the FGF-2-treated group, gelatin hydrogel sheets containing 5 µg of rhFGF-2 (Kaken Pharmaceutical Co., Tokyo, Japan) were applied. All rats were sacrificed at 2, 4, 6, 8, or 12 weeks postoperatively. At each time point, 6 specimens per group were used for histological evaluation (i.e., histology, immunohistochemistry, or *in situ* hybridization), and 6 per group were analyzed with real-time reverse transcription polymerase chain reaction (RT-PCR). At 6 and 12 weeks, 9 specimens per group were used for biomechanical testing.

Local Administration of FGF-2

110   We used a biodegradable gelatin hydrogel sheet[21] (MedGel PI5, MedGEL Co) as a carrier for

111   the FGF-2. In our pilot study, three doses of FGF-2 (0.5, 5, and 50 μg/site) in gelatin hydrogel sheets

112   were compared between the carrier-only and suture-only groups using the same method in the

113   present study (n = 6 per group underwent histological and biomechanical testing). At 12 weeks

114   postoperatively, a significant improvement in the ultimate load-to-failure was achieved in all

115   FGF-2-treated groups (0.5-μg, 29.1 ± 10.1 N; 5-μg, 31.7 ± 8.5 N; and 50-μg, 25.9 ± 8.6 N) compared

116   to the carrier-only (15.8 ± 4.5 N) and suture-only groups (12.4 ± 2.4 N). The histological scores in

117   the FGF-2-treated groups (0.5-μg, 9.7 ± 1.0; 5-μg, 10.7 ± 0.5; and 50-μg, 10.3 ± 0.5) were higher

118   than that in the suture-only (7.5 ± 0.5) and carrier-only groups (7.8 ± 0.8). Although there were no

119   significant differences among the three FGF-2-treated groups, we used the 5-μg dose of FGF-2,

120   because the 5-μg FGF-2-treated group showed the highest histological score and the ultimate

121   load-to-failure.

122   Before administration, freeze-dried gelatin hydrogel sheets (1 mg) for each shoulder were soaked

123   with 10 μL of a PBS or FGF-2 (500 μg/mL), and the sheets were incubated for 60 min at room

124   temperature (RT).

125

126   **Surgical Procedure**

127   The rats underwent left shoulder surgery, as previously described.[6, 23] Briefly, after the

128   administration of general anesthesia with an intraperitoneal injection of pentobarbital (25–30 mg/kg),

129   longitudinal antero-lateral skin and deltoid muscle incisions were made, and the supraspinatus

130   tendon was exposure. The supraspinatus tendon was detached sharply at its insertion (3 mm in the

131   anterior-to-posterior dimension), and the fibrocartilaginous stump on the greater tuberosity was

132   completely removed using a high-speed bur until bleeding was observed. A 0.8-mm drill hole was

133   created transversely in an anterior-posterior orientation through the proximal part of the humerus. We

134   sutured the torn supraspinatus tendon to its anatomic position using a double-armed 5-0 prolene

135   suture (Ethicon, Somerville, NJ) using a modified Mason-Allen method. A gelatin hydrogel sheet

136   soaked with PBS or FGF-2 was fixed to the torn end of the tendon using a 5-0 prolene suture, which

137   is used for repair, and it was secured between the tendon and bone. The incision was closed in layers

138   with 4-0 nylon sutures. All rats were permitted cage activities without immobilization

139   postoperatively.

140

141   **Biomechanical Testing**

142   As previously described,[9, 26] 9 animals per group were tested at 6 and 12 weeks postoperatively,

143   and 9 intact shoulders were used as a normal control. All specimens were frozen at -80°C until

144   testing. After thawing, the supraspinatus tendon repair to the humerus was dissected from the

145   surrounding tissues with a custom-designed double scalpel blade to a 2-mm-width to standardize the

146   tendon tested, and the supraspinatus muscle belly and any scar tissue was removed. Each specimen

147   was preloaded to 0.1 N and loaded to failure with a conventional tensile tester (STA1225; Orientec,

148   Tokyo, Japan) at a rate of 10 mm/min, and the ultimate load-to-failure and the failure site were

149   recorded. The linear region of the load-displacement curve was used to calculate the stiffness. The

150   cross-sectional area of the repaired insertion site, including its width and thickness, was measured

151   using a digital micro-caliper.[7] The ultimate load-to-failure was divided by the cross-sectional area of

152   the repair site to determine the ultimate stress-to-failure.

153

154   **Histological Evaluation**

155   The tissues were fixed overnight in 4% paraformaldehyde at an abduction angle of 30° and were

156   decalcified in Morse's solution (10% sodium citrate and 22.5% formic acid). After decalcification,

157   the tissues were dehydrated and were embedded in paraffin. The sections were viewed under an

158   Olympus BX-51 microscope (Olympus Optical, Tokyo, Japan), and digital images were taken using

159   a DP70 camera (Olympus Optical). To evaluate healing at the tendon-to-bone site semi-quantitatively,

160   we used a computerized image analysis (Image J, National Institutes of Health, Bethesda, MD) and a

161   modified scoring system (Table 1) based on previously reported histological evaluations.[24, 26, 28] We

162   scored the healing insertion site according to three histological parameters (i.e., cellularity,

163   vascularity, and collagen fiber orientation). Three sequential sections were obtained from each

164   animal for each staining, and the results were averaged.

165   To analyze cellularity, all cell nuclei in a randomly selected region of interest (200 × 200 μm) were

166   counted to calculate the number per mm^2 at the insertion site (100–400 μm proximal to the bone

167   trough) on hematoxylin and eosin (HE)-stained slides under 100-fold magnification.

168   To analyze vascularity, all blood vessels were counted to calculate the mean vessel number from

169   three sequential sections at the insertion site (100–400 μm proximal to the bone trough) on

170   HE-stained slides under 100-fold magnification.

171   The collagen fiber orientation was assessed by picrosirius-red stained sections using a polarizing

172   microscope.[7, 26] On eight-bit digitized images, intense white areas of brightly diffracted light on a

173   gray scale (black, 0; white, 255), were observed. Higher gray scales indicated more organized

174   collagen fibers. We randomly selected 10 square areas (100 × 100 μm) at the insertion site (100–400

175   μm proximal to the bone trough) under 12.5-fold magnification, and gray scales were measured

176   using Image J. The values from the 10 areas were averaged to obtain a value of average gray scales

177   per specimen. To reduce sampling errors, we took photomicrographs of three sequential sections

178   from each specimen under the same illumination conditions.

179   Cellularity and collagen fiber orientation were scored using the percentage of the value measured

180   in six right shoulders (intact side). A perfect score is 12 points (Table 1). Analysis was performed by

181   two colleagues who were blinded to the groups for each specimen and the time points throughout the

182   histological examinations.

183

Immunohistochemistry

184

185   Semi-serial sections (4 μm) were prepared for immunostaining. To assess the cell proliferation, the

186   expression of Sox9 and existence of MSCs, we performed immunostaining for PCNA and Sox9 at all

187   time points, MSC-related surface antigens (CD105, CD90, and CD73), and hematopoietic cell

188   antigen (CD45 and CD34) at 2 and 4 weeks postoperatively.[2]

189   The sections were deparaffinized; rehydrated; and incubated overnight at 4°C with a primary

190   antibody recognizing PCNA (dilution 1:200, clone PC10; Dakopatts, Copenhagen, Denmark), Sox9

191   (1:200, AB5535; Millipore, Billerica, MA), CD105 (1:50,#05-1424; Millipore), CD90 (1:200,

192   AB225; Abcam, Cambridge, MA), CD73 (1:200, AB175396; Abcam), CD45 (1:1000, AB10558;

193   Abcam), and CD34 (1:100, AB 64480; Abcam). Subsequent reactions were performed using a

194   peroxidase-labeled antibody (Histofine Simple Stain Max PO; Nichirei, Tokyo, Japan), which

195   reacted with a 3, 3-diaminobenzidine solution and were counterstained in 0.5% Mayer's

196   hematoxylin.

197

Estimation of Cell Proliferation and the Expression of Sox9 at the Healing Site

198

199   To estimate cell proliferation at the healing site, we modified the previously described method for

200   PCNA-positive cell counting.[12] Three square areas (200 × 200 μm) at the insertion site (100–400 μm

201   proximal to the bone trough) were selected randomly under 200-fold magnification. The percentage

202   of PCNA-positive cells was calculated by dividing the number of PCNA-positive cells by the total

203   number of cells in the area; the average percentage of three areas from each slide was recorded.

204   The percentage of Sox9-positive cells was calculated in the same manner.

205

206   **RNA Isolation and Real-time Reverse Transcription Polymerase Chain Reaction Analysis**

207   At all time points, the left (operative side) and right (intact side) tendon-to-bone tissues were

208   dissected and flash frozen in liquid nitrogen and crushed using a Multi-beads Shocker (Yasui Kikai,

209   Osaka, Japan). After homogenization, total RNA was extracted and purified per the manufacturer's

210   instructions using the TRIzol Plus RNA Purification Kit (Invitrogen, Carlsbad, CA). The total RNA

211   (1 µg) was reverse transcribed to complementary DNA (cDNA) using the Thermoscript RT kit

212   (Invitrogen). Real-time PCR was performed using an ABI7500 system (Applied Biosystems, Foster,

213   CA) with TaqMan Universal PCR Master Mix and TaqMan™ Gene Expression Assays for the

214   following genes: *Scx* (Assay ID: Rn01504576_m1), *Tnmd* (Rn00574164_m1), *Sox9*

215   (Rn01751069_mH), and *18S ribosomal RNA* (Rn03928990_g1). Each sample was analyzed in

216   duplicate. The relative expression levels for the target genes were analyzed using the comparative Ct

217   method. The delta-Ct values were calculated by the difference between the Ct values of the target

218   genes and *18S ribosomal RNA*. The results are represented as the relative gene expression compared

219   to the intact tendon.[16]

220

14

221 ***In situ* Hybridization**

222   *In situ* hybridization was performed to detect the expression of *Scx* and *Tnmd* mRNA as previously

223 described.[1] Briefly, 5-µm sections were deparaffinized, rehydrated, incubated with proteinase K (20

224 µg/mL; Gibco BRL, Rockville, MO), post-fixed in 4% paraformaldehyde, acetylated with 0.1 M

225 triethanolamine containing 0.25% acetic anhydride for 10 min, dehydrated, and air-dried.

226   Sense and antisense RNA probes labeled with digoxigenin (DIG) for *Scx* or *Tnmd* were

227 synthesized by *in vitro* transcription with a DIG RNA labeling kit (Roche, Mannheim, Germany)

228 using the following cDNA clones: rat *Scx* cDNA containing a 0.726 kb fragment was subcloned into

229 pBSII SK+ (Stratagene, La Jolla, CA) and rat *Tnmd* cDNA containing a 0.607 kb fragment was

230 subcloned into pCRII-TOPO (Invitrogen), as a template after linearization. Hybridization was

231 performed at 50°C for 16 h. After hybridization, the sections were washed in $2 \times$ SSC containing

232 50% formamide, treated with RNase A (20 µg/mL), and washed in $2 \times$ SSC. Immunological probe

233 detection was performed with an anti-DIG-AP Fab fragment (Roche) and BM Purple (Roche). The

234 specificity of these antisense probes was confirmed on mouse embryo (E16.5) sections as positive

235 controls. Sense probes for *Scx* and *Tnmd* were used on sections as negative controls.

236

237 **Evaluation of the Association between the Locations of Reparative Tissue Accompanying**

238 **Collagen Fibers with an Aligned Orientation and *Scx* or *Tnmd* mRNA**

239   To investigate the correlation between the location of healing tissues with aligned collagen fiber

240   orientation and the localization of *Scx* or *Tnmd* mRNA, images from picrosirius-red staining and *in*

241   *situ* hybridization in sections in the treatment and control groups at 8 weeks postoperatively (n = 12)

242   were evaluated, and nine areas (tendon, suture, and insertion areas of the articular side, middle, and

243   bursal side) were set (see Figure 5C). Collagen fiber orientation for each area was evaluated by

244   applying the gray scale as described above. Expression levels of *Scx* or *Tnmd* mRNA (density of

245   hybridization signals) in each area were graded using previously reported[23] standards to define high

246   (4), moderate (3), low (2), and undetectable (1) levels, and the highest grade for each area from each

247   specimen was recorded.

248

Statistical Analysis

250   Before the study initiation, a power analysis was performed using the G*Power 3.1 program,[5]

251   which we used in our pilot study described above that had a similar rat model. A minimum of 9

252   specimens per group for each time point was required for biomechanical testing (Cohen's d, ≥ 1.45),

253   and a minimum of 6 specimens per group for each time point was required for histological evaluation

254   (Cohen's d, ≥ 2.04), with an α value of 0.05 and a power of 0.80 based on the effect size. The sample

255   size for real-time RT-PCR was determined according to the power analysis for histological

256   evaluation. Our primary analysis compared measurements between the groups at each time point,

257   and the secondary analysis compared measurements within the groups over time. We used

258 nonparametric statistical methods for all the analyses, because the data were non-normally

259 distributed. Statistical significance between the groups at each time point was estimated using the

260 Mann-Whitney U test. Differences in the measurements within groups over time were analyzed using

261 the Kruskal-Wallis test, followed by the post-hoc Scheffe test for multiple comparisons.

262 The correlation between the collagen fiber orientation and the expression levels of *Scx* or *Tnmd*

263 mRNA were assessed using Spearman's correlation analysis. Values of $P < .05$ were considered

264 statistically significant.

265

266 **Results**

267 **Biomechanical Testing**

268   Three of 9 specimens from the normal shoulders failed at the insertion site; the other 6 failed at the

269 tendon mid-substance. All specimens from the operated groups failed at the site of surgical repair

270 (Table 2).

271   At 6 weeks postoperatively, the ultimate load-to-failure, stiffness, and ultimate stress-to-failure

272 were significantly higher in the FGF-2-treated group than in the control. No significant differences

273 were observed between the groups in the cross-sectional area of the repair site.

274   At 12 weeks postoperatively, the ultimate load-to-failure and ultimate stress-to-failure were

275 significantly higher in the FGF-2-treated group than in the control. No significant differences were

276 observed between the groups in the stiffness and cross-sectional area of the repair site.

277

278 **Histological Analysis**

279 **Effects of FGF-2 on the histological appearance**

280   At 2 weeks postoperatively, hyper-cellular and hyper-vascular granulations were noted in the

281 insertion site (Figure 1A, G), and areas of brightly diffracted polarized light were rarely observed at

282 the insertion site in any of the groups (Figure 1D, J).

283   From 6 to 12 weeks, although granulations decreased compared to the previous time point, the

284 tendon-to-bone area remained hyper-vascular and filled with disorganized collagen fibers in the

285   controls (Figure 1B, C, E, F). Conversely, in the FGF-2-treated groups, these granulations were

286   decreased, and the area of brightly diffracted polarized light at the insertion site was larger than that

287   in the controls (Figure 1H, I, K, L). The histological differences between the treatment and control

288   group were observed at ≥4 weeks.

289   At the bone surface, normal fibrocartilaginous enthesis was not regenerated in any specimen from

290   any group at any time point.

291   In both groups, cellularity and vascularity decreased, but the collagen fiber orientation and total

292   histological scores increased with time (Table 3). The mean number of blood vessels at the insertion

293   site was significantly smaller in the FGF-2-treated group than in the control at 8 and 12 weeks

294   postoperatively. Collagen fiber orientation and the total score were significantly higher in the

295   FGF-2-treated group than in the control at ≥4 weeks.

296

297   **Effects of FGF-2 on cell proliferation**

298   At 2 and 4 weeks postoperatively, greater numbers of PCNA-positive cells were observed in the

299   granulation tissue between the tendon and bone in the FGF-2-treated group than those in the control

300   (Figure 2A, C). At ≥6 weeks, PCNA-positive cells obviously decreased and were mainly present at

301   the bone surface in both groups (Figure 2E). The percentage of PCNA-positive cells was

302   significantly larger in the FGF-2-treated group than in the control at 2 weeks (45.4 ± 9.3% vs. 30.8 ±

303   5.7%; $P = .016$) and 4 weeks (41.9 ± 8.0% vs. 29.0 ± 7.4%; $P = .025$). There were no differences

304   between the groups at 6 weeks (control, $21.2 \pm 4.6\%$; FGF-2-treated, $23.8 \pm 5.3\%$; $P = .423$), 8

305   weeks (control, $19.7 \pm 2.7\%$; FGF-2-treated, $22.3 \pm 5.7\%$; $P = .263$) and 12 weeks (control, $19.0 \pm$

306   3.8%; FGF-2-treated, $19.6 \pm 5.3\%$; $P = .749$) (Figure 2E).

307

308   **Effect of FGF-2 on the expression of *Scx* and *Tnmd***

309   Real-time RT-PCR analysis showed that a significantly higher expression of *Scx* was detected in

310   the FGF-2-treated group than in the control at 4, 6, and 8 weeks ($P = .010, .010$, and $.004$,

311   respectively). There were no differences between the control and FGF-2 groups at 2 and 12 weeks (P

312    $= .631$, and $.150$, respectively) (Figure 3A). *Tnmd* expression was significantly higher in the

313   FGF-2-treated group than in the control at 4, 6, 8, and 12 weeks ($P = .004, .010, .004$, and $.016$,

314   respectively). There were no differences between the groups at 2 weeks ($P = .631$) (Figure 3B). *Scx*

315   expression was transiently upregulated from 4 to 8 weeks; meanwhile *Tnmd* expression was

316   persistently upregulated by FGF-2 treatment even after 12 weeks postoperatively (Figure 3).

317   We then performed *in situ* hybridization to analyze the localization of *Scx* and *Tnmd* mRNA. In

318   both groups, hybridization signals for *Scx* were detected in the spindle-shaped cells at the tendon

319   mid-substance at all time points (Figure 4A, C, I, K), and a few hybridization signals for *Scx* were

320   detected in the round and spindle-shaped cells within the granulation tissue around the suture at 4, 6,

321   and 8 weeks (data not shown). In the control, hybridization signals for *Scx* were rarely detected

322   within the fibro-vascular tissue at the bone surface at any time points (Figure 4E, G). However, in the

20

323   FGF-2-treated group, *Scx* were expressed in the spindle-shaped cells at the bone surface at ≥4 weeks

324   (Figure 4M, O).

325   *Tnmd* signals were also detected in the spindle-shaped cells at the tendon mid-substance in both

326   groups at all time points, and hybridization signals increased with time (Figure 4B, D, J, L). In the

327   FGF-2-treated group, the distribution of these signals expanded into reparative tissues near the

328   suturing site compared to the control. However, *Tnmd* was rarely detected at the bone surface in

329   either group at any time point (Figure 4F, H, N, P).

330

331   **Correlation between the locations of healing tissue with aligned collagen fiber orientation and**

332   ***Scx* or *Tnmd* mRNA**

333   We assessed 108 areas in both groups at 8 weeks postoperatively (Figure 5). A weak positive

334   correlation between the location of aligned collagen fiber orientation and expression levels of *Scx*

335   mRNA in each area was observed (Spearman's rank correlation [ρ] = .27, *P* < .001) (Figure 5D).

336   Meanwhile, a strong positive correlation between the location of aligned collagen fiber orientation

337   and the expression levels of *Tnmd* mRNA in each area was observed (ρ = .88, *P* < .001) (Figure 5E).

338

339   **Effect of FGF-2 on Sox9 expression**

340   Real-time RT-PCR analysis showed that *Sox9* expression was significantly higher in the

341   FGF-2-treated group than in the control at 4 weeks (*P* = .004). However, at 2, 6, 8 and 12 weeks,

21

342   there were no statistically significant differences between the groups (P = .337, .749, .200 and, .337,

343   respectively) (Figure 6).

344   In immunostaining for Sox9 (Figure 7), Sox9-positive cells were mainly observed at the

345   tendon-to-bone insertion site, but a few Sox9-positive spindle-shaped cells were also detected at the

346   tendon mid-substance at ≥ 4 weeks in both groups. The percentage of Sox9-positive cells was

347   significantly higher in the FGF-2-treated group than in the control at 4 weeks (23.7 ± 4.9% vs. 14.0 ±

348   3.6%; P = .010). There were no differences between the groups at 2 weeks (control, 10.1 ± 4.8%;

349   FGF-2-treated, 13.4 ± 6.6%; P = .337), 6 weeks (control, 19.7 ± 2.7%; FGF-2-treated, 22.3 ± 5.7%;

350   P = .263), 8 weeks (control, 10.3 ± 1.1%; FGF-2-treated, 11.2 ± 1.5%; P = .423), and 12 weeks

351   (control, 10.1 ± 2.6%; FGF-2-treated, 11.3 ± 3.4%; P = .749) (Figure 7I).

352

353   **Effect of FGF-2 on mesenchymal stem cells marker-positive cells in the early phase of healing**

354   To analyze MSCs, serial sections were immunostained for MSC-related surface antigens (CD105,

355   CD90, and CD73) and hematopoietic cell antigen (CD45 and CD34) at 2 and 4 weeks

356   postoperatively. CD45- and CD34-positive cells were rarely detectable at the insertion site in either

357   group. In the FGF-2-treated group, cells positive for CD105, CD90, and CD73 were detected more

358   within the reparative tissue at the insertion site than in the control (Figure 8).

Discussion

359

360   Our findings support our hypothesis that FGF-2 stimulates the tenogenic differentiation of

361   progenitors to improve the biomechanical strength and histological appearance of repaired RCs in

362   rats. Previous studies[6, 23] have described the healing response as observed using histological

363   evaluation in a rat RC acute injury and immediate repair model, and the healing response occurred

364   almost exclusively within the tendon-to-bone insertion site that was filled with hyper-cellular and

365   hyper-vascular granulation tissues by postoperative day 10. As healing progresses, cellularity and

366   vascularity decrease, and then the improvement of collagen fiber orientation and fiber integration

367   into the bone were observed to some extent. However, a histologically normal tissue is not

368   regenerated. Instead, the disorganized fibro-vascular scar interposes at the insertion site without

369   supplementation of growth/differentiation factors.[23] Without FGF-2 administration, in this study, the

370   fibro-vascular scar interposes between the tendon and bone even 12 weeks after RC repair surgery.

371   In contrast, the administration of FGF-2 clearly decreased the occurrence of fibro-vascular scarring

372   at the insertion site and increased the aligned orientation of collagen fibers at ≥4 weeks, as indicated

373   by significantly higher histological scores (Figure 1, Table 3). Moreover, even though normal

374   biomechanical strength was not achieved at 12 weeks postoperatively (ultimate load-to-failure,

375   56.7% of normal controls; stiffness, 33.3% of normal controls; ultimate load-to-stress, 35.1% of

376   normal controls), FGF-2 administration significantly increased the biomechanical strength by 6

377   weeks postoperatively (Table 2). In an ovine study model on tendon-to-bone healing, the

378   disorganized fibro-vascular scar at the insertion site was weaker than the axially-aligned collagen

379   fibers in the bone.[8] These results suggest that the improvement of mechanical strength by FGF-2

380   treatment is associated with decreases in the fibro-vascular scarring and improvement in the collagen

381   fiber orientation at the insertion site.

382   Accumulating evidence suggests that *Scx*-expressing tenogenic cells can participate in a

383   regenerative repair of tendons to promote the formation of collagen fibers with an aligned orientation,

384   which have better tensile strength. Gulotta et al.[7] demonstrated that application of bone

385   marrow-derived MSCs transduced with *Scx* resulted in an improvement in histological and

386   biomechanical properties at 4 weeks postoperatively in a similar rat RC healing model. Tan et al.[22]

387   also reported that transplantation of *Scx*-transduced tendon-derived stem cells provided better tendon

388   repair than that of mock-transduced cells in a rat patellar tendon injury model from the histological

389   and biomechanical viewpoints.

390   Our study showed that FGF-2 administration induced *Scx* expression in the cells of healing tissue

391   4–8 weeks postoperatively, indicating that more tenogenic progenitor cells were generated at the

392   healing sites from the mid-to-late stages of healing (Figures 3–4). During differentiation from

393   tenogenic progenitors to mature tenocytes, the *Scx* expression declines, while *Tnmd* is continuously

394   expressed.[10, 18] In murine tendon development, *Scx* expression increases from E10.5 to E12.5 and

395   decreases at E13.5, meanwhile the expression of *Tnmd* sharply increases from E13.5 and persists

396   until the late stage in the forelimb tendon cells.[10] These temporal expression patterns of *Scx* and

24

397   *Tnmd* were also demonstrated in mouse patellar healing.[16] In this study, *Tnmd*-positive tenocyte-like

398   cells were persistently observed until the later stage of healing from 4–12 weeks postoperatively.

399   Interestingly, *Tnmd*-positive tenocyte-like cells were only observed in the area with highly oriented

400   collagen fibers. In particular, these cells were distributed into the reparative tissues near the suturing

401   site in the FGF-2-treated group 4–12 weeks postoperatively, which was consistent with highly

402   oriented collagen fiber areas as shown by the histological evaluation in this study (Figure 5E). These

403   spatial patterns of *Tnmd* expression are similar to that in the late-stage of tendon development,[18]

404   suggesting that *Tnmd* is a useful marker for evaluating the differentiation of mature tenocyte-like

405   cells in tendon healing.

406   Despite enhanced differentiation of *Tnmd*-positive tenocyte-like cells, it is unlikely that FGF-2

407   directly stimulated tenogenic differentiation of cells in this later phase of RC healing, since FGF-2 is

408   known to be released from gelatin hydrogel sheets within 2 weeks.[21] Thus, the FGF-2-stimulated

409   tenogenic repair responses in this study must be primarily mediated by the growth stimulation of

410   undifferentiated mesenchymal cells, as indicated by a higher incidence of PCNA-positive cells at the

411   repair sites during the early phase (Figure 2). In a mouse patellar tendon healing model,[4]

412   undifferentiated mesenchymal progenitors migrate from a paratenon to the healing site by 1 week

413   post-injury. Subsequently, *Scx*-expressing cells appear at ≥2 weeks, suggesting that the initial growth

414   of undifferentiated mesenchymal progenitors have a critical role for the subsequent tenogenic

415   differentiation of cells during the later phase of healing. In agreement with the previous *in vitro*

416   studies[11, 19, 25] that have shown that FGF-2 potently stimulates the self-renewal of MSCs and/or

417   progenitor cells without a loss of potentials for the subsequent cell differentiation, we demonstrated

418   at least in the present study that the healing process started with a better accumulation of cells

419   expressing MSC-related markers within 2 weeks in the FGF-2-treated group (Figure 8).

420   There are several limitations to the current study. First, our acutely created tear and immediate

421   repair model does not reflect chronic degenerative RC tears, and our findings in this rat model may

422   not directly translate to humans, because the healing processes in healthy animals may not mirror the

423   situations encountered in clinical practice. However, based on anatomical similarities between

424   humans, this model has been widely used to investigate the mechanism of healing[6, 23, 27] and the

425   method of healing enhancement.[7, 9, 24] Second, this study did not directly identify the function of

426   tenogenic marker genes during the RC healing process. Further studies using a knockout model on

427   *Scx* or *Tnmd* are required to determine the roles of these genes during the RC healing process. Third,

428   our findings demonstrated that the biomechanical and histological values of the control group did not

429   reach those of the FGF-2-treated group by 12 weeks. A longer time period may be necessary to

430   understand whether the effect observed in the FGF-2-treated group will persist throughout the

431   healing response. Fourth, the sample size, which was based on the large effect size, was relatively

432   small, and it may be underpowered to detect significant differences. Likewise, our histological

433   evaluation may also be underpowered, because it did not include all sections from the specimens.

434   However, there was little or no discrepancy among our findings observed in various evaluation

435   methods during RC healing. Lastly, direct clinical implications for treatment may be difficult to

436   determine from this small animal model. Currently, little is known about the biological mechanisms

437   underlying the RC healing response.[6] Therefore, basic research on these mechanisms may provide

438   clues in order to determine the safety, effect, dose, and method of administration in larger models.

439   Ultimately, human clinical trials are also needed to translate these findings to clinical use.

440   It is not known whether FGF-2 can selectively facilitate the growth of undifferentiated tenogenic

441   cells of a certain mesenchymal lineage. However, the enhanced expression of *Scx* and *Tnmd* genes in

442   the mid-to-late stages indicates that a certain microenvironment favorable for the growth response of

443   tenogenic progenitor cells to FGF-2 may be provided in the present RC healing model. Interestingly,

444   the transient upregulation of *Sox9* detected in the FGF-2-treated group at 4 weeks postoperatively

445   may indicate that a possible occurrence of *Sox9* and *Scx* double-positive tenogenic progenitors

446   contributes to enthesis formation during development.[20] Thus, further analysis of the cellular

447   components and the microenvironment at the RC repair sites will help develop clinical strategies for

448   inducing a specific regenerative healing response in RC injuries.

449

References

450

451   1.   Anraku Y, Mizuta H, Sei A, et al. Analyses of early events during chondrogenic repair in rat

452   full-thickness articular cartilage defects. *J Bone Miner Metab.* 2009;27(3):272-286.

453   2.   Chamberlain G, Fox J, Ashton B, Middleton J. Concise review: mesenchymal stem cells:

454   their phenotype, differentiation capacity, immunological features, and potential for homing.

455   *Stem Cells.* 2007;25(11):2739-2749.

456   3.   Docheva D, Hunziker EB, Fassler R, Brandau O. Tenomodulin is necessary for tenocyte

457   proliferation and tendon maturation. *Mol Cell Biol.* 2005;25(2):699-705.

458   4.   Dyment NA, Hagiwara Y, Matthews BG, Li Y, Kalajzic I, Rowe DW. Lineage tracing of

459   resident tendon progenitor cells during growth and natural healing. *PLoS One.*

460   2014;9(4):e96113.

461   5.   Faul F, Erdfelder E, Buchner A, Lang AG. Statistical power analyses using G*Power 3.1:

462   tests for correlation and regression analyses. *Behav Res Methods.* 2009;41(4):1149-1160.

463   6.   Galatz LM, Sandell LJ, Rothermich SY, et al. Characteristics of the rat supraspinatus tendon

464   during tendon-to-bone healing after acute injury. *J Orthop Res.* 2006;24(3):541-550.

465   7.   Gulotta LV, Kovacevic D, Packer JD, Deng XH, Rodeo SA. Bone marrow-derived

466   mesenchymal stem cells transduced with scleraxis improve rotator cuff healing in a rat model.

467   *Am J Sports Med.* 2011;39(6):1282-1289.

468   8.   Hee CK, Dines JS, Dines DM, et al. Augmentation of a rotator cuff suture repair using

469   rhPDGF-BB and a type I bovine collagen matrix in an ovine model. *Am J Sports Med.*

470   2011;39(8):1630-1639.

471   9.   Ide J, Kikukawa K, Hirose J, et al. The effect of a local application of fibroblast growth

472   factor-2 on tendon-to-bone remodeling in rats with acute injury and repair of the

473   supraspinatus tendon. *J Shoulder Elbow Surg.* 2009;18(3):391-398.

474   10.   Liu H, Zhang C, Zhu S, et al. Mohawk promotes the tenogenesis of mesenchymal stem cells

28

475   through activation of the TGFβ signaling pathway. *Stem Cells*. 2014;33(2):443-455.

476   11.   Lotz S, Goderie S, Tokas N, et al. Sustained levels of FGF2 maintain undifferentiated stem

477   cell cultures with biweekly feeding. *PLoS One*. 2013;8(2):e56289.

478   12.   Mizuta H, Kudo S, Nakamura E, Otsuka Y, Takagi K, Hiraki Y. Active proliferation of

479   mesenchymal cells prior to the chondrogenic repair response in rabbit full-thickness defects

480   of articular cartilage. *Osteoarthritis Cartilage*. 2004;12(7):586-596.

481   13.   Murchison ND, Price BA, Conner DA, et al. Regulation of tendon differentiation by scleraxis

482   distinguishes force-transmitting tendons from muscle-anchoring tendons. *Development*.

483   2007;134(14):2697-2708.

484   14.   Russell RD, Knight JR, Mulligan E, Khazzam MS. Structural integrity after rotator cuff

485   repair does not correlate with patient function and pain: a meta-analysis. *J Bone Joint Surg*

486   *Am*. 2014;96(4):265-271.

487   15.   Schweitzer R, Chyung JH, Murtaugh LC, et al. Analysis of the tendon cell fate using

488   Scleraxis, a specific marker for tendons and ligaments. *Development*.

489   2001;128(19):3855-3866.

490   16.   Scott A, Sampaio A, Abraham T, Duronio C, Underhill TM. Scleraxis expression is

491   coordinately regulated in a murine model of patellar tendon injury. *J Orthop Res*.

492   2011;29(2):289-296.

493   17.   Shukunami C, Oshima Y, Hiraki Y. Chondromodulin-I and tenomodulin: a new class of

494   tissue-specific angiogenesis inhibitors found in hypovascular connective tissues. *Biochem*

495   *Biophys Res Commun*. 2005;333(2):299-307.

496   18.   Shukunami C, Takimoto A, Oro M, Hiraki Y. Scleraxis positively regulates the expression of

497   tenomodulin, a differentiation marker of tenocytes. *Dev Biol*. 2006;298(1):234-247.

498   19.   Solchaga LA, Penick K, Goldberg VM, Caplan AI, Welter JF. Fibroblast growth factor-2

499   enhances proliferation and delays loss of chondrogenic potential in human adult

bone-marrow-derived mesenchymal stem cells. *Tissue Eng Part A.* 2010;16(3):1009-1019.

20. Sugimoto Y, Takimoto A, Akiyama H, et al. Scx+/Sox9+ progenitors contribute to the establishment of the junction between cartilage and tendon/ligament. *Development.* 2013;140(11):2280-2288.

21. Tabata Y, Ikada Y. Vascularization effect of basic fibroblast growth factor released from gelatin hydrogels with different biodegradabilities. *Biomaterials.* 1999;20(22):2169-2175.

22. Tan C, Lui PP, Lee YW, Wong YM. Scx-transduced tendon-derived stem cells (tdscs) promoted better tendon repair compared to mock-transduced cells in a rat patellar tendon window injury model. *PLoS One.* 2014;9(5):e97453.

23. Thomopoulos S, Hattersley G, Rosen V, et al. The localized expression of extracellular matrix components in healing tendon insertion sites: an in situ hybridization study. *J Orthop Res.* 2002;20(3):454-463.

24. Thomopoulos S, Soslowsky LJ, Flanagan CL, et al. The effect of fibrin clot on healing rat supraspinatus tendon defects. *J Shoulder Elbow Surg.* 2002;11(3):239-247.

25. Tsutsumi S, Shimazu A, Miyazaki K, et al. Retention of multilineage differentiation potential of mesenchymal cells during proliferation in response to FGF. *Biochem Biophys Res Commun.* 2001;288(2):413-419.

26. Uezono K, Ide J, Tokunaga T, et al. Effect of postoperative passive motion on rotator cuff reconstruction with acellular dermal matrix grafts in a rat model. *Am J Sports Med.* 2014;42(8):1930-1938.

27. Wurgler-Hauri CC, Dourte LM, Baradet TC, Williams GR, Soslowsky LJ. Temporal expression of 8 growth factors in tendon-to-bone healing in a rat supraspinatus model. *J Shoulder Elbow Surg.* 2007;16(5 Suppl):S198-203.

28. Yokoya S, Mochizuki Y, Natsu K, Omae H, Nagata Y, Ochi M. Rotator cuff regeneration using a bioabsorbable material with bone marrow-derived mesenchymal stem cells in a rabbit

525   model. *Am J Sports Med.* 2012;40(6):1259-1268.

526

Figure legends

528 **Figure 1:** Photomicrographs of the specimens at 2, 6 and 12 weeks postoperatively (A–F: control;

529 G–L: FGF-2-treated). The hematoxylin and eosin-stained sections (A–C, G–I) and picrosirius-red

530 stained sections under polarized light (D–F, J–L). The boxed areas in A–C and G–I are shown at a

531 higher magnification in a–c and g–i, respectively. Bars, 200 μm.

532

533 **Figure 2:** Immunostaining for the proliferating cell nuclear antigen (PCNA) at 2 and 6 weeks

534 postoperatively (A, B: control; C, D: FGF-2-treated). The sections are counterstained with

535 hematoxylin. Bars, 100 μm.

536 The percentage of PCNA-positive cells in the region of interest at the insertion site during rotator

537 cuff healing (E). Bar graphs, the mean for each group; error bars, one standard deviation. $^{*}P < .05$, **

538 $P < .01$.

539

540 **Figure 3:** The gene expression levels of *Scleraxis* (A) and *Tenomodulin* (B) in the healing tissues.

541 The target genes are normalized to *18S ribosomal RNA* expression and are further normalized to the

542 intact supraspinatus tendon tissues that are equal to 1. Bar graphs, the mean for each group; error

543 bars, one standard deviation. $^{*}P < .05$, $^{**}P < .01$.

544

545 **Figure 4:** *In situ* hybridization of *Scleraxis* and *Tenomodulin* at the tendon mid-substance (A–F,

546 M–R) and the insertion site (G–L, S–X) at 2 and 8 weeks postoperatively (A–L: control; M–X:

547 FGF-2-treated). Sense, the negative control using a sense labeled probe. Arrows, the hybridization

548 signals. Bars, 100 μm.

549

550 **Figure 5:** Picrosirius-red-stained sections under polarized light (A) and *in situ* hybridization of

551 *Tenomodulin* (B) for the FGF-2-treated group at 8 weeks postoperatively. Arrows, the hybridization

552 signals. Bars, 200 μm. Schematic illustration of the segmented area in healing tissues (C). (t, tendon

553 areas; s, suture areas; i, insertion areas; a, articular side; m, middle layer; b, bursal side).

554 Correlation between collagen fiber orientation and the expression levels of *Scx* mRNA (D), or *Tnmd*

555 mRNA (E) for each area in both groups, respectively. Gray scale percentages are relative values

556 compared to six intact specimens. The correlation coefficient (ρ) and *P*-value were obtained by

557 Spearman's correlation analysis.

558

559 **Figure 6:** The gene expression levels of *Sox9* in the healing tissues. The target genes are normalized

560 to *18S ribosomal RNA* expression and are further normalized to the intact supraspinatus tendon

561 tissues that are equal to 1. Bar graphs, the mean for each group; error bars, one standard deviation. [*]

562 $P < .05,$ [**] $P < .01.$

563

564 **Figure 7:** Immunostaining for Sox9 at 2, 4, 6, and 12 weeks postoperatively (A–D: control; E–H:

33

565   FGF-2-treated). The percentage of Sox9-positive cells in the region of interest at the insertion site

566   (G). The sections are counterstained with hematoxylin. Bars, 50 μm. Bar graphs, the mean for each

567   group; the error bars, one standard deviation. $^*P < .05$, $^{**}P < .01$.

568

569   **Figure 8:** Immunostaining for mesenchymal stem cell-related surface antigens CD105 (A, F), CD90

570   (B, G), and CD73 (C, H) and hematopoietic cell antigen CD45 (D, I) and CD34 (E, J) at the insertion

571   site at 2 weeks postoperatively. A–E (control) and F–J (FGF-2-treated) are serial sections

572   counterstained with hematoxylin. Bars, 50 μm.

573

574   Table 1

575

576

TABLE 1

The Histological Scoring System

Characteristics	Score
Cellularity (%)[a]	
> 400	1
300－400	2
200－300	3
< 200	4
Vascularity (bv/low PF)[b]	
> 15	1
10－15	2
6－10	3
< 6	4
Collagen fiber orientation (%)[c]	
< 25	1
25－50	2
50－75	3
> 75	4

[a] Number of cells per region of interest from each section; percentages represent relative values compared to the values from normal tendon-to-bone   sections (n = 6), which were set at 100%.

[b] Number of blood vessels per low PF (100-fold magnification) from each section; bv, blood vessel; PF, power field.

[c] Gray scale per region of interest from each section as measured using Image J, percentages represent relative values compared to the values from normal tendon-to-bone   sections (n = 6), which were set at 100%.

577   Table 2

578

579

TABLE 2

The Summary of The Biomechanical Testing[a]

Time point group	Ultimate load-to-failure (N)	Stiffness (N/mm)	Cross-sectional area (mm^2)	Ultimate stress-to-failure (N/mm^2)
6 weeks				
Control (n = 9)	7.92 ± 2.54 ⎤*	3.43 ± 1.24 ⎤*	3.53 ± 0.51	2.34 ± 0.93 ⎤*
FGF-2 (n = 9)	15.1 ± 3.32 ⎦	7.16 ± 3.28 ⎦	3.56 ± 0.35	4.24 ± 0.96 ⎦
P value	.009	.005	.627	.001
12 weeks				
Control (n = 9)	13.8 ± 4.69[b] ⎤*	6.83 ± 1.25[b]	3.53 ±0.26	3.88 ± 1.12[b] ⎤*
FGF-2 (n = 9)	23.8 ± 4.61[b] ⎦	8.98 ± 3.58	3.42 ±0.28	6.92 ± 1.10[b] ⎦
P value	.003	.310	.354	.003
Normal control (n = 9)	42.0 ± 5.56	27.0 ± 2.85	2.09 ± 0.13	19.7 ± 2.44

[a]All values are the mean ± standard deviation.
[b]Significantly different between time points within group ($P <$ .05).
*Significantly different between groups at the same time point ($P <$ .01).

TABLE 3

Summary of The Histological Assessment [a]

Time point Treatment	Cellularity[b] (%)	Vascularity[c] (bv/ low PF)	Collagen fiber orientation[d] (%)	Total score[e]
2 weeks				
Control (n = 6)	552 ±72.5	35.7 ±8.4	17.9 ±2.5	3.0 ±0.0
FGF-2 (n = 6)	604 ±98.3	44.7 ±8.7	21.6 ±3.7	3.2 ±0.4
P value	.423	.109	.078	.631
4 weeks				
Control (n = 6)	448 ±56.9	31.5 ±3.4	41.4 ±10.9[f] ⎤*	4.0 ±0.6 ⎤*
FGF-2 (n = 6)	503 ±30.8	29.9 ±9.2[f]	56.0 ±3.3[f] ⎦	4.8 ±0.4 ⎦
P value	.078	.689	.007	.045
6 weeks				
Control (n = 6)	447 ±49.1 ⎤*	22.7 ±5.5[f]	57.4 ±5.3[f] ⎤*	5.2 ±0.4[f,g] ⎤*
FGF-2 (n = 6)	377 ±41.2[f,g] ⎦	18.4 ±5.7[f]	68.1 ±4.8[f,g] ⎦	6.3 ±1.0[f] ⎦
P value	.025	.298	.025	.037
8 weeks				
Control (n = 6)	389 ±41.2[f]	21.6 ±6.6[f] ⎤*	62.5 ±4.6[f,h] ⎤*	5.8 ±0.4[e,f] ⎤*
FGF-2 (n = 6)	338 ±59.0[e,f]	11.4 ±4.7[f,g] ⎦	73.4 ±8.1[f,g] ⎦	8.0 ±1.7[e,f] ⎦
P value	.128	.020	.025	.013
12 weeks				
Control (n = 6)	350 ±57.2[e]	13.6 ±3.3[f,g] ⎤*	70.8 ±6.4[f,h] ⎤*	7.2 ±1.0[f,i] ⎤*
FGF-2 (n = 6)	288 ±52.5[f,g]	8.1 ±2.3[f,g] ⎦	81.9 ±4.5[f,h] ⎦	9.3 ±1.2[f,h] ⎦
P value	.109	.013	.025	.013

[a] All values are the mean ± standard deviation.

[b] Number of cells per region of interest from each section; percentages represent relative values compared to the values from normal tendon-to-bone sections (837 ± 86.3 cells/mm2, n = 6), which were set to 100%.

[c] Number of blood vessels per low PF (100-fold magnification) from each section; bv, blood vessel; PF, power field.

[d] Gray scale per region of interest from each section as measured using Image J; percentages represent relative values compared to the values from normal tendon-to-bone sections (191.0 ± 17.5 gray scale, n = 6), which were set to 100%.

[e] Scores represent a total score of three parameters including cellularity, vascularily and collagen fiber orientation. A perfect score in this scoring system is 12 points.

[f-i] Significantly different within group compared to 2(f), 4(g), 6(h), and 8 weeks(i), respectively ($P < .05$).

*Significantly different between groups at the same time point ($P < .05$).
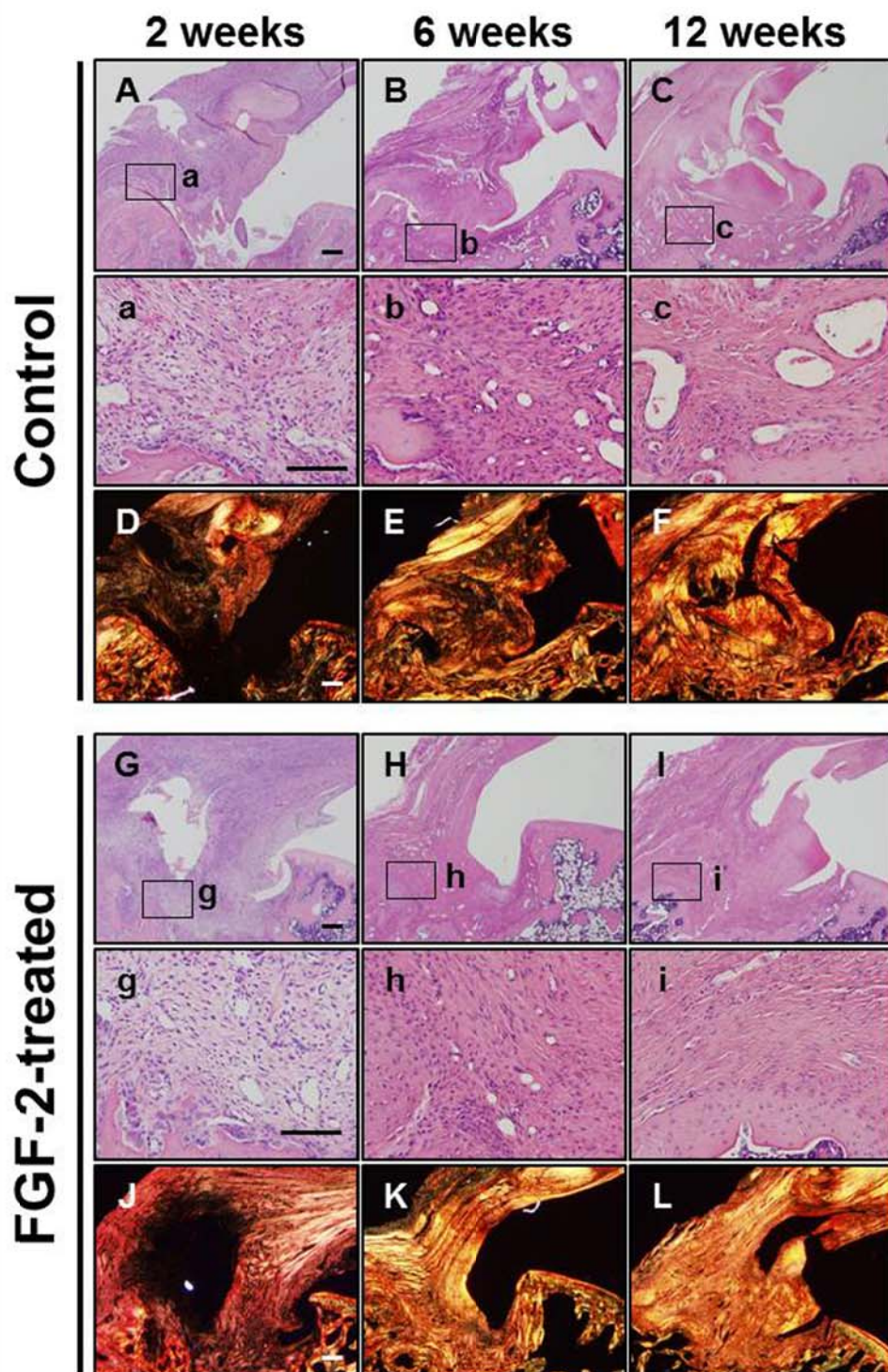
Figure 1. Photomicrographs of the specimens at 2, 6 and 12 weeks postoperatively (A–F: control; G–L: FGF-2-treated). The hematoxylin and eosin-stained sections (A–C, G–I) and picrosirius-red stained sections under polarized light (D–F, J–L). The boxed areas in A–C and G–I are shown at a higher magnification in a–c and g–i, respectively. Bars, 200 μm.
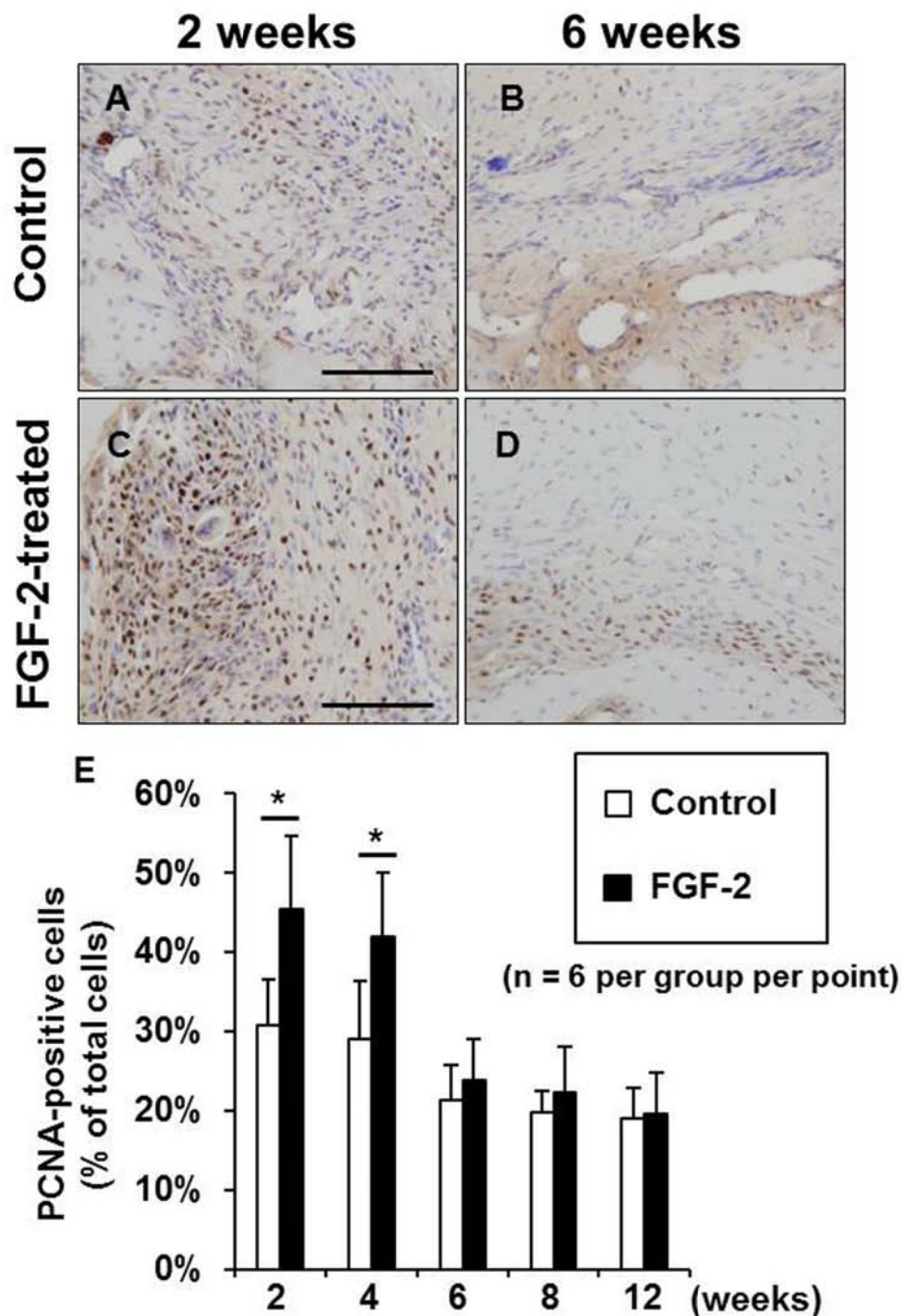
Figure 2. Immunostaining for the proliferating cell nuclear antigen (PCNA) at 2 and 6 weeks postoperatively (A, B: control; C, D: FGF-2-treated). The sections are counterstained with hematoxylin. Bars, 100 μm.

The percentage of PCNA-positive cells in the region of interest at the insertion site during rotator cuff healing (E). Bar graphs, the mean for each group; error bars, one standard deviation. $^*P < .05$, $^{**}P < .01$.
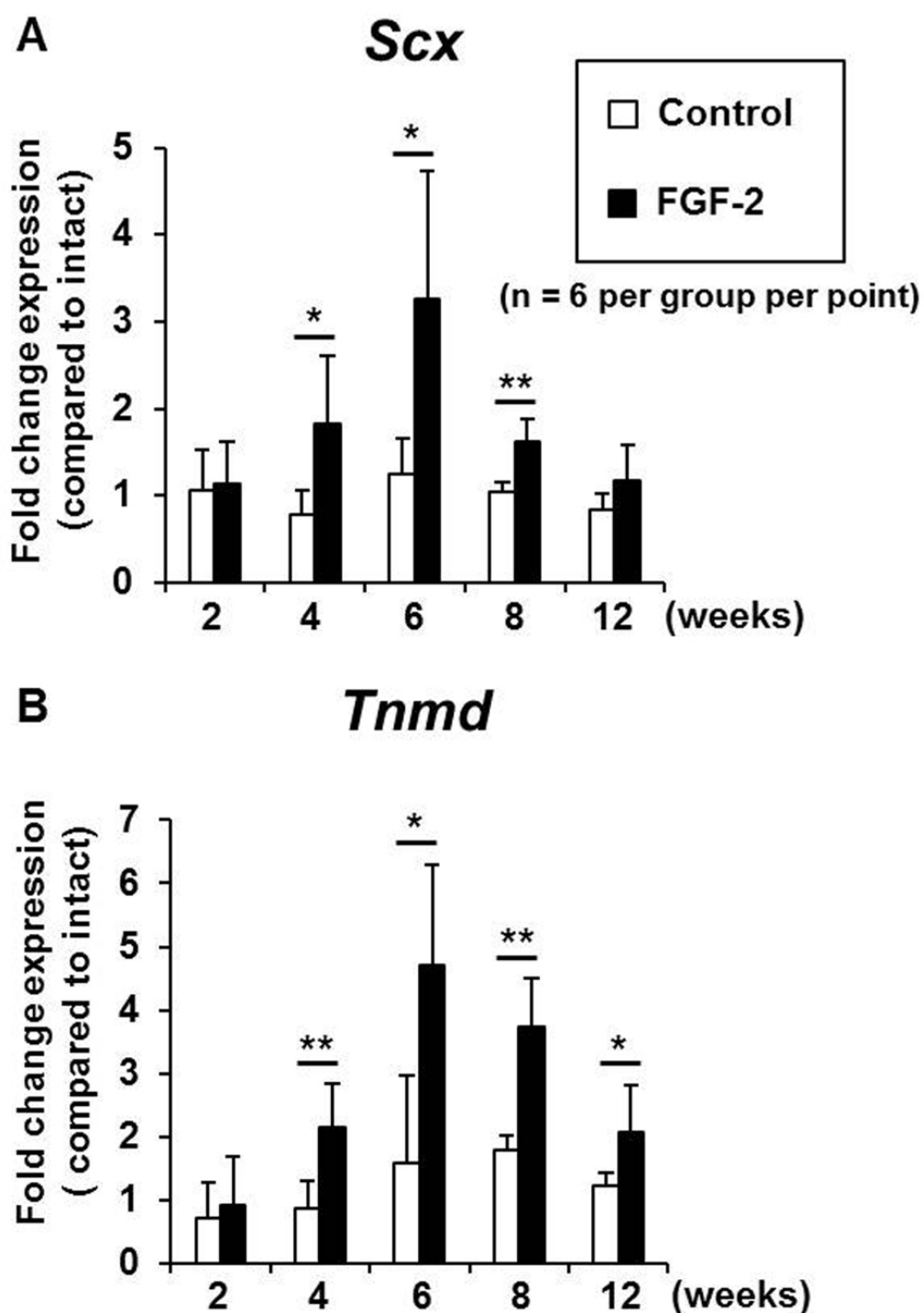
Figure 3. The gene expression levels of *Scleraxis* (A) and *Tenomodulin* (B) in the healing tissues. The target genes are normalized to *18S ribosomal RNA* expression and are further normalized to the intact supraspinatus tendon tissues that are equal to 1. Bar graphs, the mean for each group; error bars, one standard deviation. $^{*}P < .05$, $^{**}P < .01$.
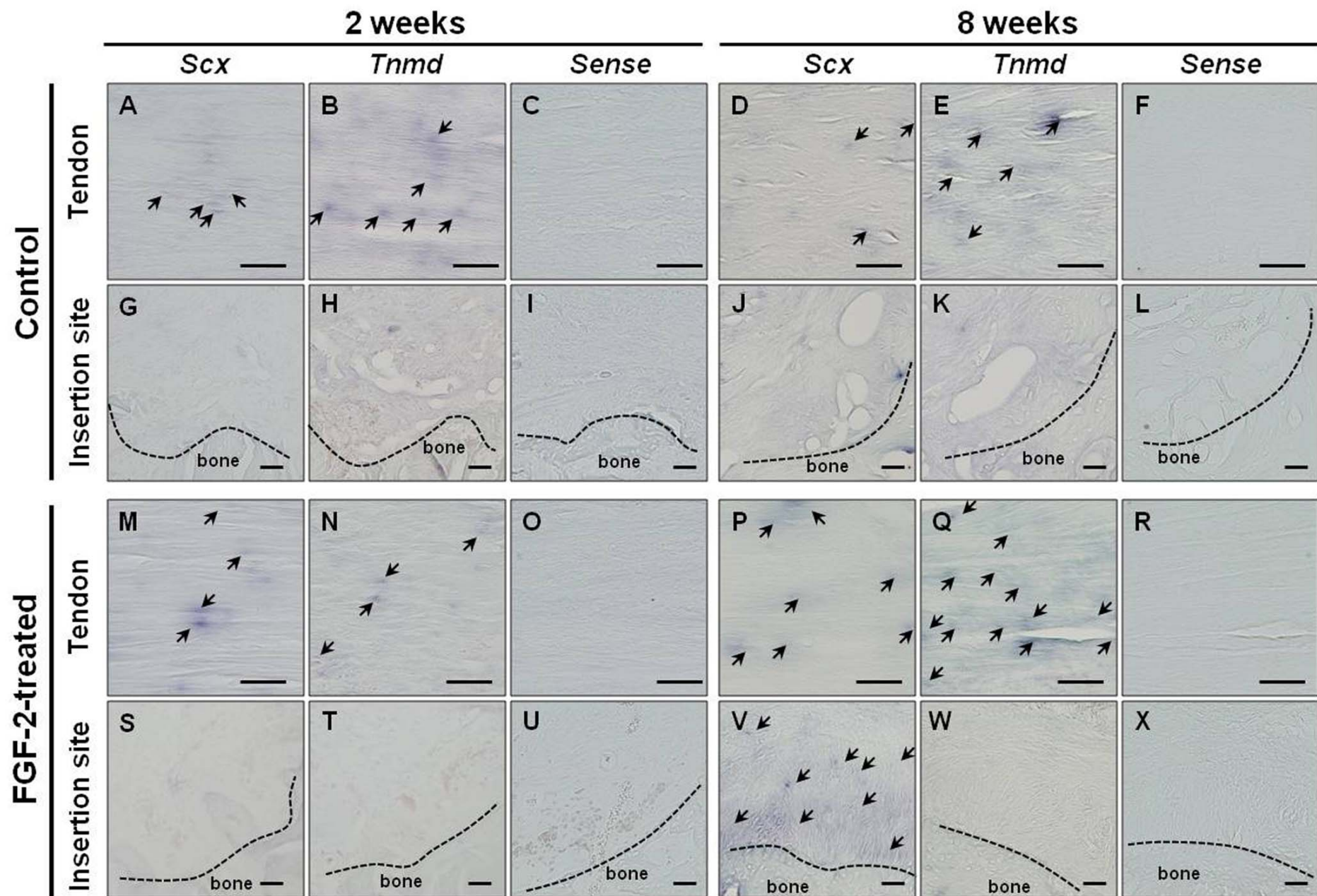
Figure 4. *In situ* hybridization of *Scleraxis* and *Tenomodulin* at the tendon mid-substance (A–F, M–R) and the insertion site (G–L, S–X) at 2 and 8 weeks postoperatively (A–L: control; M–X: FGF-2-treated). Sense, the negative control using a sense labeled probe. Arrows, the hybridization signals. Bars, 100 μm.
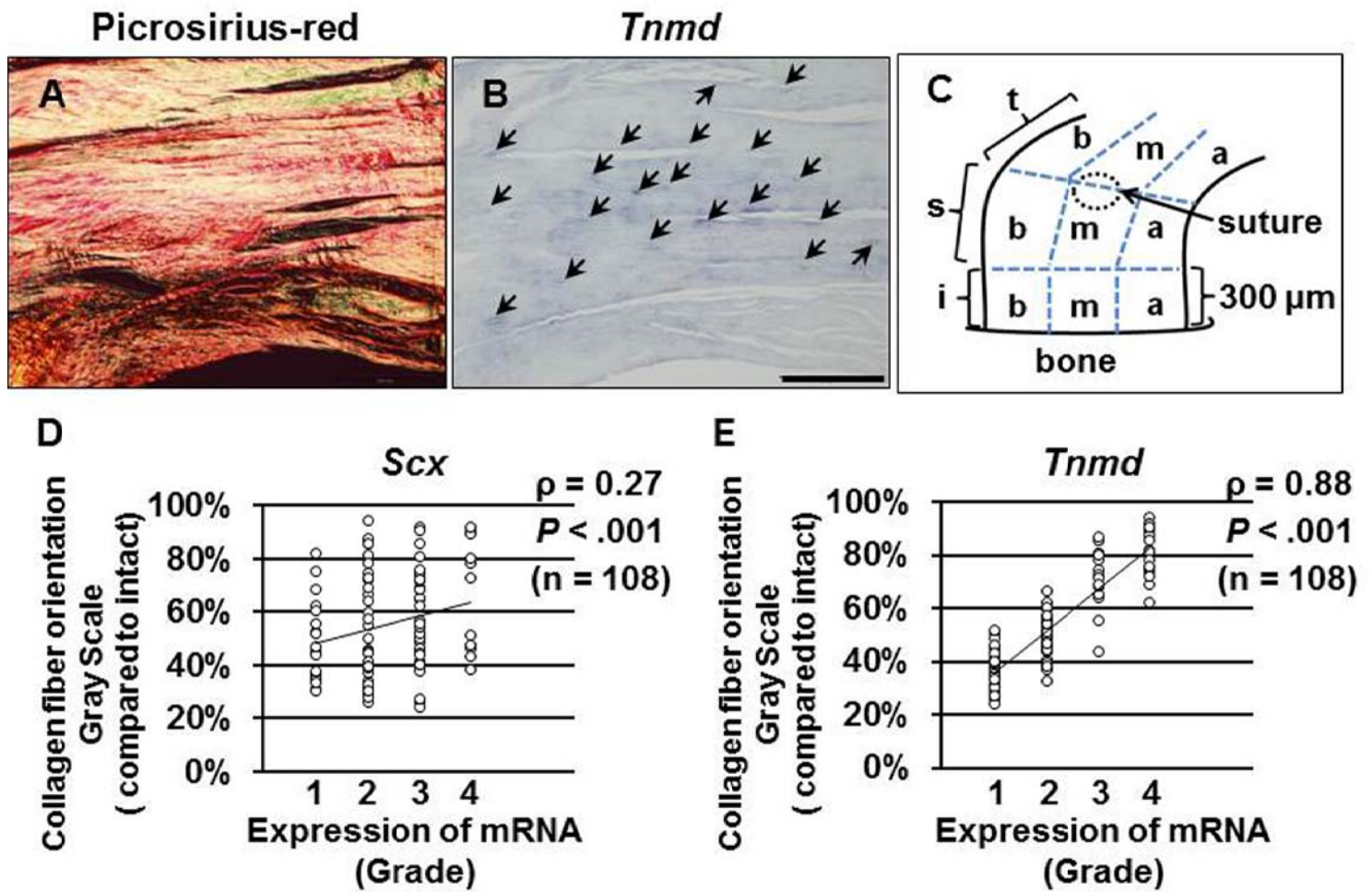
Figure 5. Picrosirius-red-stained sections under polarized light (A) and *in situ* hybridization of *Tenomodulin* (B) for the FGF-2-treated group at 8 weeks postoperatively. Arrows, the hybridization signals. Bars, 200 μm. Schematic illustration of the segmented area in healing tissues (C). (t, tendon areas; s, suture areas; i, insertion areas; a, articular side; m, middle layer; b, bursal side). Correlation between collagen fiber orientation and the expression levels of *Scx* mRNA (D), or *Tnmd* mRNA (E) for each area in both groups, respectively. Gray scale percentages are relative values compared to six intact specimens. The correlation coefficient (ρ) and *P*-value were obtained by Spearman's correlation analysis.
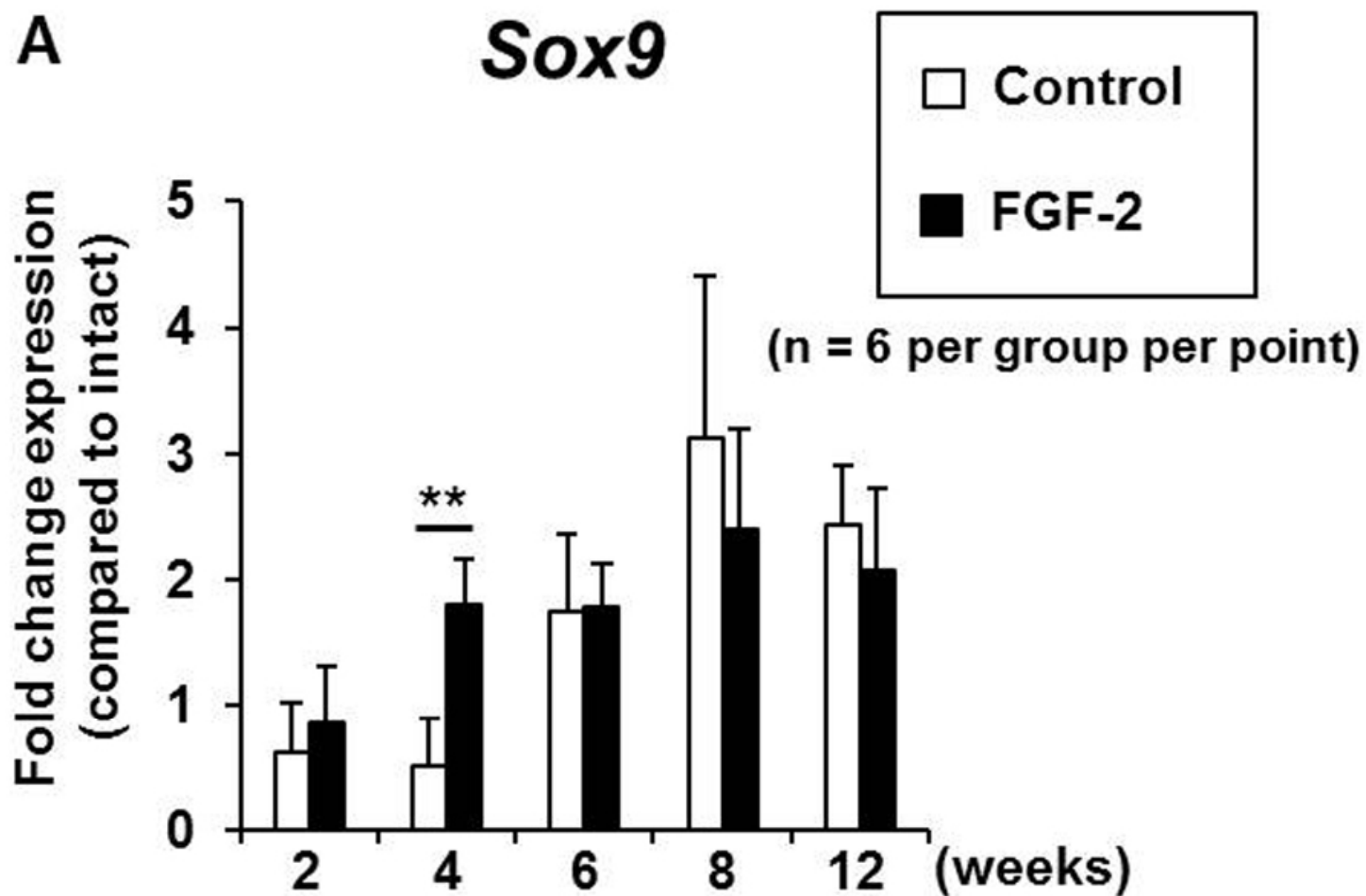
Figure 6. The gene expression levels of *Sox9* in the healing tissues. The target genes are normalized to *18S ribosomal RNA* expression and are further normalized to the intact supraspinatus tendon tissues that are equal to 1. Bar graphs, the mean for each group; error bars, one standard deviation. $^{*}P < .05$, $^{**}P < .01$.
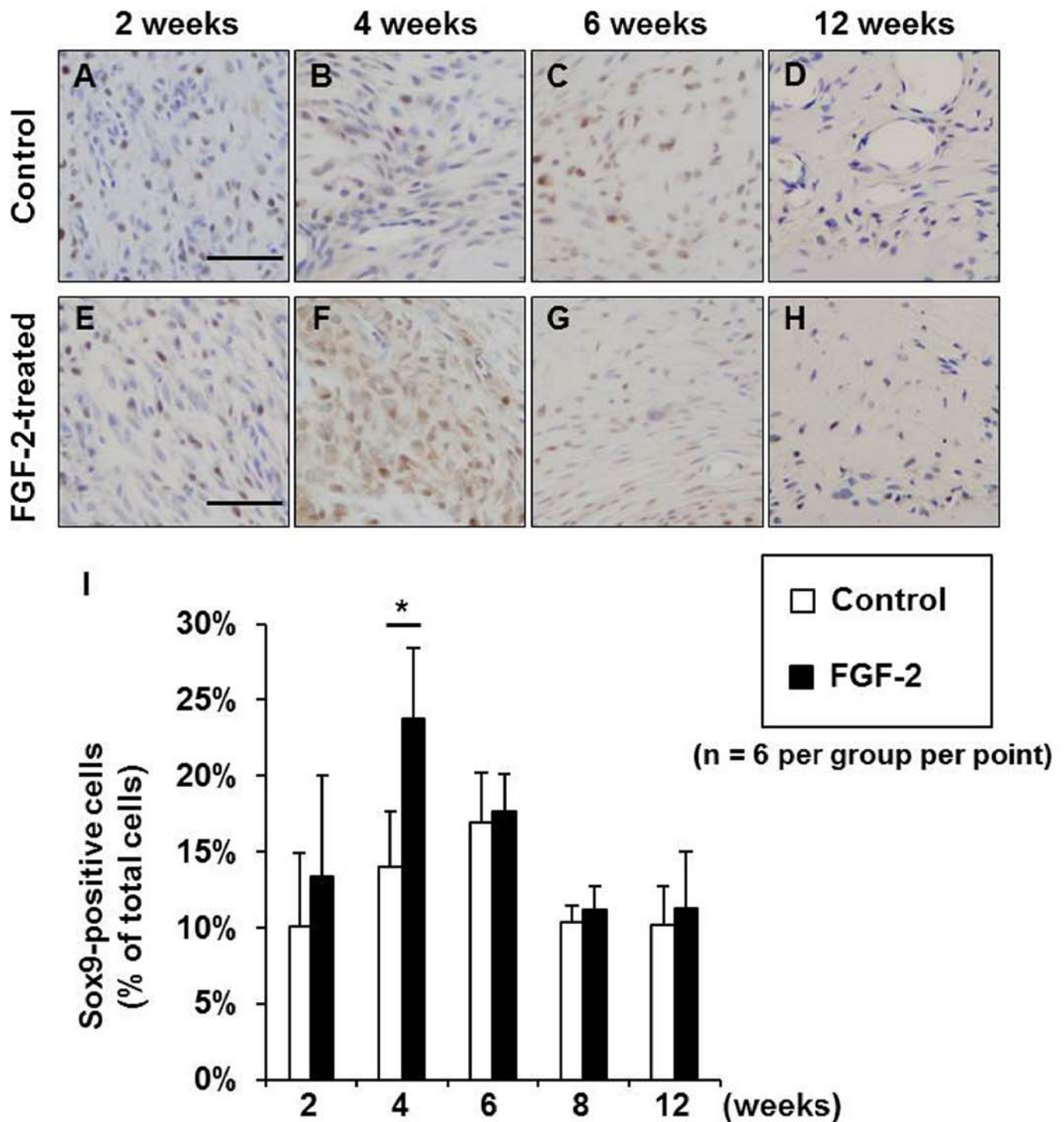
Figure 7. Immunostaining for Sox9 at 2, 4, 6, and 12 weeks postoperatively (A–D: control; E–H: FGF-2-treated). The percentage of Sox9-positive cells in the region of interest at the insertion site (G). The sections are counterstained with hematoxylin. Bars, 50 μm. Bar graphs, the mean for each group; the error bars, one standard deviation. $^{*}P < .05$, $^{**}P < .01$.
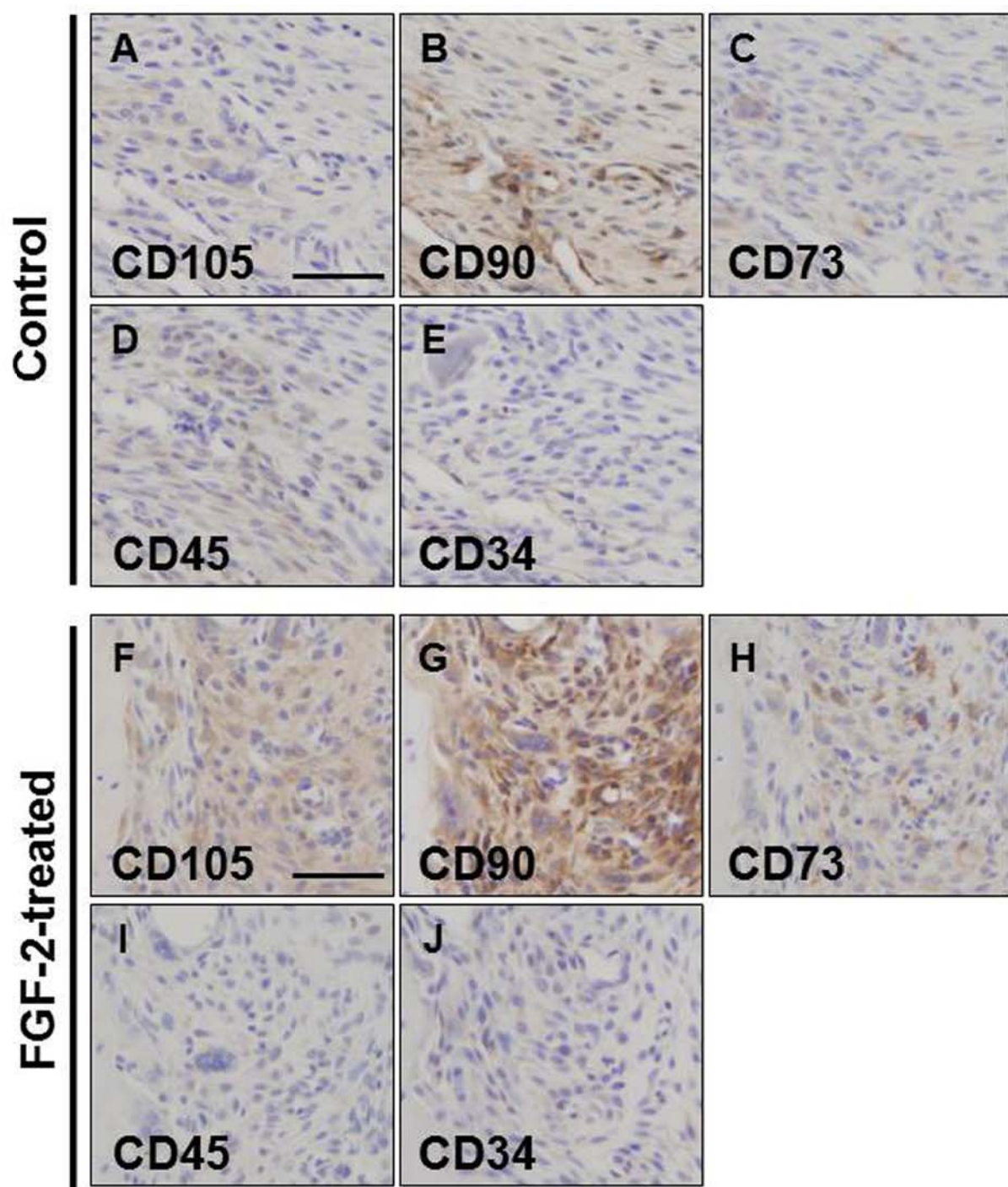
Figure 8. Immunostaining for mesenchymal stem cell-related surface antigens CD105 (A, F), CD90 (B, G), and CD73 (C, H) and hematopoietic cell antigen CD45 (D, I) and CD34 (E, J) at the insertion site at 2 weeks postoperatively. A–E (control) and F–J (FGF-2-treated) are serial sections counterstained with hematoxylin. Bars, 50 μm.